AWARD NUMBER: W81XWH-17-1-0525

TITLE: Iron Chelation Enhances TAM and Triple Negative Breast Cancer Cell Death

PRINCIPAL INVESTIGATOR: Jason Koutcher

CONTRACTING ORGANIZATION: Sloan Kettering Institute for Cancer Research
New York, NY 10065-6007

REPORT DATE: October 2020

TYPE OF REPORT: Annual

PREPARED FOR: U.S. Army Medical Research and Development Command
Fort Detrick, Maryland 21702-5012

REPORT DOCUMENTATION PAGE

Form Approved
OMB No. 0704-0188

1. REPORT DATE	2. REPORT TYPE	3. DATES COVERED
Oct 2020	Annual	9/15/2019- 9/14/2020

4. TITLE AND SUBTITLE
Iron Chelation Enhances TAM and Triple Negative Breast Cancer Cell Death

5a. CONTRACT NUMBER

5b. GRANT NUMBER
W81XWH-17-1-0525

5c. PROGRAM ELEMENT NUMBER

6. AUTHOR(S)
Jason Koutcher

E-Mail: koutchej@mskcc.org

5d. PROJECT NUMBER

5e. TASK NUMBER

5f. WORK UNIT NUMBER

7. PERFORMING ORGANIZATION NAME(S) AND ADDRESS(ES)
Sloan Kettering Institute for Cancer Research
1275 York Avenue, New York, NY 10065-6007

8. PERFORMING ORGANIZATION REPORT NUMBER

9. SPONSORING / MONITORING AGENCY NAME(S) AND ADDRESS(ES)
U.S. Army Medical Research and Development Command
Fort Detrick, Maryland 21702-5012

10. SPONSOR/MONITOR'S ACRONYM(S)

11. SPONSOR/MONITOR'S REPORT NUMBER(S)

12. DISTRIBUTION / AVAILABILITY STATEMENT
Approved for Public Release; Distribution Unlimited

13. SUPPLEMENTARY NOTES

14. ABSTRACT The goal of this study is preclinical testing of Deferiprone (DFP), an iron chelator in clinical use for non-oncologic diseases. The IC50 for tumor cells was lower than measured for macrophages (M0, M1, M2)indicating potential therapeutic gain and safety in treating cancer cells. In 4T1 tumors, we observed significantly smaller spleens in both size and weight in the DFP alone, cisplatin and paclitaxel groups treated with DFP. We found an increase in the spleen in percent of both CD4 effector T cells (CD4+ Foxp3-)and CD8 T cells and an increase in the ability of CD4 and CD8 T cells to make both IFNγ or TNFα. In perfused 4T1 cells, we demonstrated metabolic inhibition of the tricarboxylic acid cycle in the MDA-231. WE have measured changes in oxygen consumption rate in 4T1 and MDA231 cells and macrophages and found changes in response to DFP.

15. SUBJECT TERMS
Breast cancer, iron imaging, MRI, metabolism, cytokines, immune effects, deferiprone, CD4, CD8

16. SECURITY CLASSIFICATION OF:			17. LIMITATION OF ABSTRACT	18. NUMBER OF PAGES	19a. NAME OF RESPONSIBLE PERSON
a. REPORT	b. ABSTRACT	c. THIS PAGE			USAMRMC
Unclassified	Unclassified	Unclassified	Unclassified	26	19b. TELEPHONE NUMBER *(include area code)*

TABLE OF CONTENTS

1. INTRODUCTION:

The goal of this study is preclinical testing of Deferiprone (DFP), an iron chelator in clinical use for nononcologic diseases. We propose to demonstrate the sensitivity of TNBC to DFP as a single agent, and in combination with immune modulation therapy (checkpoint inhibitors) and chemotherapy (paclitaxel and cisplatin). Studies were planned to be performed sequentially by first studying in vitro effects of DFP, followed by in vivo effects, and the effects of adding paclitaxel (taxol), cisplatin, and checkpoint inhibitors. We also measure the immune effects of DFP on cells (in vitro) and organs (ex vivo) including tumors.

2. KEYWORDS:

Breast cancer, iron imaging, MRI, metabolism, cytokines, immune effects, deferiprone, CD4, CD8

3. ACCOMPLISHMENTS:

What were the major goals of the project?

List the major goals of the project as stated in the approved SOW. If the application listed milestones/target dates for important activities or phases of the project, identify these dates and show actual completion dates or the percentage of completion.

Aim 1 Determine how inhibition of iron metabolism and OXPHOS impedes TAM function and metabolism, and reduces proliferation of macrophages and TNBC cells.

Aim 2: *Develop and validate non-invasive MRI methods to quantitatively and spatially monitor tumor and tissue iron and TAM infiltration, to detect changes induced by macrophage focused therapy*.

Aim 3: *Determine if inhibition of iron metabolism, TCA cycle, and OXPHOS by DFP: i) inhibits tumor growth, and ii) enhances responses to chemotherapy and immune checkpoint inhibitors in orthotopic TNBC*

What was accomplished under these goals?

For this reporting period describe: 1) major activities; 2) specific objectives; 3) significant results or key outcomes, including major findings, developments, or conclusions (both positive and negative); and/or 4) other achievements. Include a discussion of stated goals not met. Description shall include pertinent data and graphs in sufficient detail to explain any significant results achieved. A succinct description of the methodology used shall be provided. As the project progresses to completion, the emphasis in reporting in this section should shift from reporting activities to reporting accomplishments.

Aim 1 – We previously reported the effects of DFP on metabolism in the 4T1 TNBC cell line. During this year we have recently completed 1) studies on the changes in MDA-MB-231 metabolism (**Koutcher Lab**) 2) to complement (as proposed) these studies, we performed studies on both the 4T1 and MDA-MB-231 cells, in addition to macrophages (normal cells) measuring changes in oxygen consumption induced by DFP (**Blasberg and Koutcher Labs**), 3) the effect of DFP on T cells, immune function (cytokine production), and senescence (**Blasberg and Koutcher lab**). This has been the main focus of Year 3. We were hampered by the absence of one lab member for 6 months due to COVID 19, COVID illness in the laboratory, in addition to the laboratory being closed for longer than 2 months. The goal of these studies was to determine the effect on immune function, metabolism and oxygen consumption induced by DFP in both tumor and normal cells. These results summarized in detail on the attached sheets following this page.

The research summary is written in three separate parts to enhance clarity of the rationale, methods and data.

Immune Cell Studies and Cytokine Stimulation (Blasberg Laboratory)

Background: BALB/c mice were implanted with 10^6 4T1 cells (in 100ul) subcutaneously into the mammary fat pad. Approximately ten days later when tumors were ~50-100 mm^3 in size, animals were treated with Deferirprone (DFP) (150 mg/kg Monday – through Friday), cisplatin (4mg/kg ip weekly), cisplatin + DFP, or paclitaxel (25mg/kg; 2x/week)(+/- DFP). Spleens and tumors were harvested 8 days following the initial treatment and processed for flow cytometry. 4T1 bearing animals develop splenomegaly over time due to the expansion of myeloid derived suppressor cells (MDSCs)[1, 2]. It is recognized that addition of treatment with certain chemotherapies can selectively deplete these cells from the spleen and other tissues and enhance response[1]. Other studies suggest enhancement of immune response post cytotoxic therapy including paclitaxel[3, 4].

Results: We observed significantly smaller spleens in both size and weight in the DFP alone and the cisplatin group treated with DFP (Fig. 1A, left). Both paclitaxel groups also had significantly smaller spleens. We found an increase in the percent of both CD4 effector T cells (CD4+ Foxp3-) and CD8 T cells as a frequency of total immune cells (CD45+) in the control and cisplatin groups treated with DFP (Fig. 1A, center and right). In addition, both paclitaxel groups showed also a significant increase in these T cell populations, showing that DFP enhances T cell populations in the spleen. In all the treated groups, we observed a decrease in a subpopulation of CD4 T cells that do not express Foxp3 but express high levels of the T cell inhibitory receptor PD-1 ($4PD1^{hi}$, Fig 1B, left). This population was shown to be immunosuppressive and can be modulated in response to immune checkpoint blockade in mice and humans[5]. This decrease led to a corresponding increase in both the ratios of CD4 and CD8 to $4PD^{1hi}$ cells indicating a shift towards a pro-inflammatory environment and a decrease in immune suppressive cells (Fig 1B center and right). In the small sample size, a decrease in the weight of the tumors was also noted (data not shown)

Intracellular Cytokine Stimulation: Single cell suspensions of spleens and tumors were re-stimulated ex vivo with PMA and Ionomycin for 5 hours to induce cytokine production in the presence of Brefeldin A and monensin to inhibit export from the Golgi apparatus. We found an increase with DFP in the frequency of CD4 and CD8 T cells in the spleen that make either IFN□ and/or TNF□ alone or in combination with cisplatin (Fig. 2A,B), suggesting enhanced T cell effector cytokine function in response to DFP. Paclitaxel alone increased expression of these cytokines but did not have any additional benefit in combination with DFP. Additionally, with DFP, there was an increase in the ability of CD4 and CD8 T cells to make both IFN□ or TNF□ (Fig. 2C, left), a marker of polyfunctionality in T cells[6]. Similar findings were observed in the tumors especially within the CD4 T cells (Fig. 2C, right). The presence of these polyfunctional T cells correlated inversely with both spleen and tumor weight indicating a positive role in these cells in controlling tumor growth (Fig 2C).

We hypothesize that tumors from mice that progress while receiving certain chemotherapies might be immunosuppressed as a consequence of the chemotherapy, although this is likely to be tumor and drug dependent. We did not observe any significant changes in T cell frequencies in tumors (as a percentage of live CD45+ cells) or total numbers in the tumors of any of the treated animals relative to the control (data not shown). However, we did observe changes in the differentiation and activation states of the T cells within the tumors. There was a decrease in effector memory (T-EM, defined as CD44+CD62L-) CD8 T cells which was coupled with an increase in the long-lived central memory (T-CM defined as CD44+CD62L+) CD8 T cells (Fig. 3A). While effector memory cells are very good effector cells, they tend to be short lived and can represent the exhausted T cells. Central memory T cells are general more long lived and are capable of proliferating and repopulating the effector memory T cells upon antigen stimulation. Exhausted or immunosuppressed T cells often show an increase in their surface expression of T cell inhibitory receptors such as Lag-3, Tim-3 and PD-1. In addition, T cells that co-express 2 or more of these exhaustion markers are thought to the most exhausted and dysfunctional[7, 8]. We found that cisplatin alone or paclitaxel alone induces CD8 T cells in the tumor to increase co-expression of Tim-3 and PD-1 (Fig 3B). Importantly, this effect was partially reversed when DFP was added to the chemotherapy regimens. This data indicated that while chemotherapies such as cisplatin or paclitaxel can lead to T cell exhaustion as a mechanism of resistance, DFP can partially abrogate this effect and restore T cell function. The cytokine data in Fig. 2 supports this supposition.

Conclusion: In the spleen, treatment with DFP (+/- cisplatin) decreased spleen size, increased the percent of both CD4 effector T cells (CD4+ Foxp3-) and CD8 T cells, and decreased CD4 T cells that do not express Foxp3 but express high levels of the T cell inhibitory receptor PD-1. Cytokine stimulation showed that DFP the number of CD4 and CD8 T cells in the spleen that make either IFNγ and/or TNFα alone or in combination, with cisplatin. Paclitaxel alone increased

expression of these cytokines but did not have any additional benefit in combination with DFP. With DFP, there was an increase in the ability of CD4 and CD8 T cells to make both IFNγ or TNFα, a marker of polyfunctionality in T cells[6]. Similar findings were observed in the tumors especially within the CD4 T cells. These polyfunctional T cells correlated inversely with both spleen and tumor weight indicating a positive role in these cells in controlling tumor growth. We showed that cisplatin or paclitaxel can lead to tumor T cell exhaustion as a mechanism of resistance, but DFP can partially abrogate this effect and restore T cell function.

References

1. Bosiljcic M, Cederberg RA, Hamilton MJ, LePard NE, Harbourne BT, Collier JL, Halvorsen EC, Shi R, Franks SE, Kim AY, Banath JP, Hamer M, Rossi FM, Bennewith KL. Targeting myeloid-derived suppressor cells in combination with primary mammary tumor resection reduces metastatic growth in the lungs. Breast Cancer Res. 2019;21(1):103. Epub 2019/09/07. doi: 10.1186/s13058-019-1189-x. PubMed PMID: 31488209; PubMed Central PMCID: PMCPMC6727565.

2. Youn JI, Nagaraj S, Collazo M, Gabrilovich DI. Subsets of myeloid-derived suppressor cells in tumor-bearing mice. J Immunol. 2008;181(8):5791-802. Epub 2008/10/04. doi: 10.4049/jimmunol.181.8.5791. PubMed PMID: 18832739; PubMed Central PMCID: PMCPMC2575748.

3. Galluzzi L, Buque A, Kepp O, Zitvogel L, Kroemer G. Immunological Effects of Conventional Chemotherapy and Targeted Anticancer Agents. Cancer Cell. 2015;28(6):690-714. Epub 2015/12/19. doi: 10.1016/j.ccell.2015.10.012. PubMed PMID: 26678337.

4. Wanderley CW, Colon DF, Luiz JPM, Oliveira FF, Viacava PR, Leite CA, Pereira JA, Silva CM, Silva CR, Silva RL, Speck-Hernandez CA, Mota JM, Alves-Filho JC, Lima-Junior RC, Cunha TM, Cunha FQ. Paclitaxel Reduces Tumor Growth by Reprogramming Tumor-Associated Macrophages to an M1 Profile in a TLR4-Dependent Manner. Cancer Res. 2018;78(20):5891-900. Epub 2018/08/15. doi: 10.1158/0008-5472.CAN-17-3480. PubMed PMID: 30104241.

5. Zappasodi R, Budhu S, Hellmann MD, Postow MA, Senbabaoglu Y, Manne S, Gasmi B, Liu C, Zhong H, Li Y, Huang AC, Hirschhorn-Cymerman D, Panageas KS, Wherry EJ, Merghoub T, Wolchok JD. Non-conventional Inhibitory CD4(+)Foxp3(-)PD-1(hi) T Cells as a Biomarker of Immune Checkpoint Blockade Activity. Cancer Cell. 2018;33(6):1017-32 e7. Epub 2018/06/13. doi: 10.1016/j.ccell.2018.05.009. PubMed PMID: 29894689; PubMed Central PMCID: PMCPMC6648657.

6. Malandro N, Budhu S, Kuhn NF, Liu C, Murphy JT, Cortez C, Zhong H, Yang X, Rizzuto G, Altan-Bonnet G, Merghoub T, Wolchok JD. Clonal Abundance of Tumor-Specific CD4(+) T Cells Potentiates Efficacy and Alters Susceptibility to Exhaustion. Immunity. 2016;44(1):179-93. Epub 2016/01/21. doi: 10.1016/j.immuni.2015.12.018. PubMed PMID: 26789923; PubMed Central PMCID: PMCPMC4996670.

7. Jones RB, Ndhlovu LC, Barbour JD, Sheth PM, Jha AR, Long BR, Wong JC, Satkunarajah M, Schweneker M, Chapman JM, Gyenes G, Vali B, Hyrcza MD, Yue FY, Kovacs C, Sassi A, Loutfy M, Halpenny R, Persad D, Spotts G, Hecht FM, Chun TW, McCune JM, Kaul R, Rini JM, Nixon DF, Ostrowski MA. Tim-3 expression defines a novel population of dysfunctional T cells with highly elevated frequencies in progressive HIV-1 infection. J Exp Med. 2008;205(12):2763-79. Epub 2008/11/13. doi: 10.1084/jem.20081398. PubMed PMID: 19001139; PubMed Central PMCID: PMCPMC2585847.

8. Sakuishi K, Apetoh L, Sullivan JM, Blazar BR, Kuchroo VK, Anderson AC. Targeting Tim-3 and PD-1 pathways to reverse T cell exhaustion and restore anti-tumor immunity. J Exp Med. 2010;207(10):2187-94. Epub 2010/09/08. doi: 10.1084/jem.20100643. PubMed PMID: 20819927; PubMed Central PMCID: PMCPMC2947065.

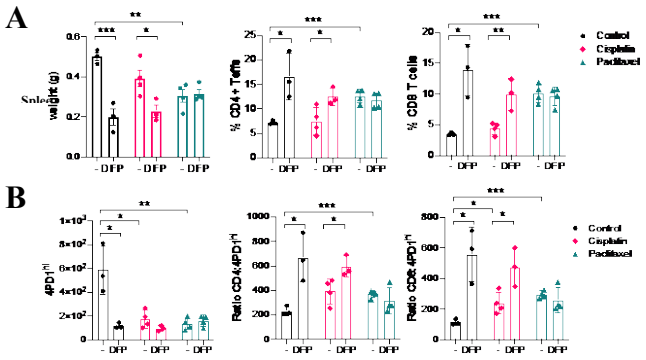

Figure 1: The combination of DFP and chemotherapy led to T cell activation in the spleen and tumor. Spleens and tumors were harvested 8 days after initial treatment with each therapy and processed for flow cytometry. **A.** Weight and frequencies of CD4 and CD8 T cells as a percent of total live CD45+ cells in the spleen. **B.** CD4+ PD-1hi T cells ($4PD1^{hi}$) normalized per gram of

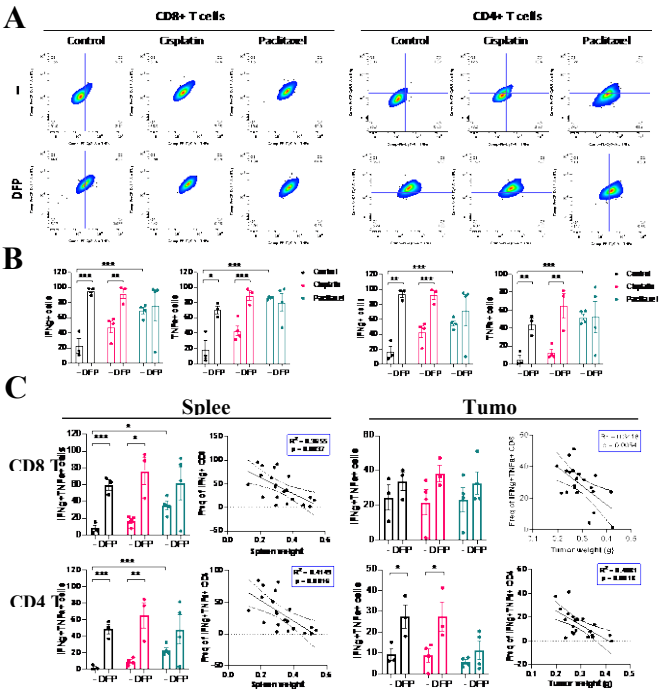

Figure 2: The combination of DFP and chemotherapy enhanced T cell cytokine production in the spleen and tumor. Spleens and tumors were harvested 8 days after initial treatment with each therapy and processed for flow cytometry. Single cells suspensions were stimulated with PMA and Ionomycin then processed for intracellular cytokines. **A.** Representative bivariate plots of TNFa vs. IFNg expressed by CD8 and CD4 T cells in the spleen. **B.** Bar graphs represent the percent of IFNg+ and TNFa+ T cell populations. **C.** The percent of IFN□ and TNF□ double positive (polyfunctional) CD8 and CD4 T cells in the spleen (left) and tumor

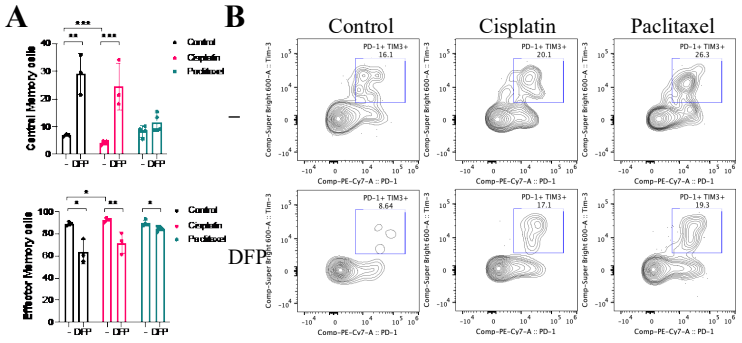

Figure 3: The combination of DFP and chemotherapy led to T cell activation in the spleen and tumor. Tumors were harvested 8 days after initial treatment and processed for expression of T cell activation and exhaustion markers. **A.** The percent of central and effector memory CD8 T cells in the tumors. **B.** Representative bivariate FACS plots of PD-1 vs. Tim-3 expression by CD8 T cells in the tumors of treated animals. * p<0.05, **p<0.01, ***p<0.005.

Effect of DFP on Oxygen Consumption of Tumor Breast Cells (Koutcher and Blasberg laboratories)

The focus of oxygen consumption rate (OCR) measurements has been to measure the effect of DFP on triple negative breast tumor (TNBC) cells, specifically the effect of DFP on basal and maximal respiration as a measure of oxygen utilization and its possible relation to metabolism at the cellular level. As macrophages are an important part of the tumor stroma, playing a significant role in tumor progression and regression, OCR measurements of a macrophage cell line were included in these experiments.

Methods

We evaluated the mitochondrial response to Deferiprone (DFP), an iron chelator, in 2 triple negative breast cancer cell lines, the human MDA-MB-231 and murine 4T1, as well as a macrophage cell line RAW264.7, polarized (M1, M2) and unpolarized (M0), by measuring the oxygen consumption rate (OCR) using the Seahorse XF Cell Mito Stress Test Kit (Agilent, Santa Clara, CA) on a Seahorse XFe96 flux analyzer (Agilent), following the manufacturer's instructions. This assay assesses mitochondrial function by measuring in live cells the effects of the sequential exposure to Oligomycin (Oligo; inhibition of ATP synthase), Carbonyl cyanide-p-trifluoromethoxyphenylhydrazone (FCCP; protonophore, uncoupler of mitochondrial oxidative phosphorylation) and Rotenone & Antimycin A (Rot/AA; inhibition of mitochondrial complexes III & I respectively) on cellular OCR (**Fig. 1A**). From the OCR measurements, 8 quantitative parameters are derived (**Fig. 1A**): Non-mitochondrial oxygen consumption (Non-Mito OC), Basal Respiration (Basal Resp), Proton Leak, ATP Production (ATP Prod), Maximal Respiration (Max Resp), Spare Respiratory Capacity (SRC), % Spare Respiratory Capacity (% SRC), and % Coupling Efficiency (% CE).

All cell lines were cultured in high-glucose Dulbecco's modified essential medium (DMEM HG), supplemented with 10% fetal calf serum, 100 U/ml Penicillin, 100 µg/ml Streptomycin and 2 mM glutamine, bringing the final glutamine concentration to 6 mM glutamine, at 37 °C in 5% CO_2 in a humidified incubator. Based on previous data [9], a 48 h exposure time to 100 µM DFP (~EC_{90} for most cell lines) was chosen. Cells were seeded 1 day prior to DFP exposure on a Seahorse XF96 V3 PS Cell Culture Microplate (Agilent) to facilitate cell attachment.

In 3 preliminary pilot experiments, cell seeding densities and assay acquisition parameters were optimized. Final cell seeding densities were 40k, 6k, 1.7k, and 7k for MDA-MB-231, RAW264.7, untreated 4T1, and DFP-treated 4T1 respectively. An additional group of untreated, unpolarized RAW264.7 at 4k seeding density was included to confirm that the observation of the lack of cell seeding density effect in RAW264.7 cells, due to cell density saturation at time of the flux analyzer measurements for seeding densities above 6k, was not further seen. The RAW264.7 cells were polarized to M2 by exposure to 20 ng/ml IL-4 for 48 h and to M1 by exposure to 100 ng/ml LPS for 48 h (>12 h exposure time for IL-4 or LPS are needed for significant polarization). The optimized acquisition parameters were 3 repeat measurements

(cycles) / assay injection stage, a 3 min mixing time and a 2 min measurement/cycle. Three experiments at optimized conditions for each of the 5 cell types were performed in addition to the pilot experiments.

After the XFe96 flux analyzer measurements, the total cell number / well and the total cell number in the sensor area of the Seahorse flux analyzer measurements (centered ~55% of total well area) as well as total protein / well were measured to facilitate normalization of the OCR measurements in each single well. Well images depicting the cell layer (**Fig. 1B**) were acquired by using the direct cell counting protocol on a Celigo Imaging Cytometer (Nexcelom Bioscience, Lawrence, MA) with a customized Seahorse XFe96 plate layout. Total cell numbers for each entire well and the sensor area (area between the posts in the well) were obtained by adjusting the analysis parameters for each cell line separately, due to their differences in contrast and cell shape (**Fig. 1B**). Of note is that 4T1 cells have a tendency, when confluent, to come off and fold over at well edges, potentially confounding the cell count. Thus, counting cells in the sensor area only alleviates the impact of an inhomogeneous cell distribution on the OCR curve normalization. Here, this was overall less of an issue, as cells were – by design – all at high confluence (>80%) at the time of the Seahorse analyzer experiment. Total protein, historically considered the gold standard for normalization of OCR curves, was measured by Pierce™ BCA Protein Assay Kit (Thermo Fisher Scientific, Waltham, MA) as described previously [9, 10]. Total protein is assumed to be directly proportional to cell number. However, this might not be true for all cell lines and might differ between cells lines, as well as be affected by treatments, Hence, we also evaluated the normalization by cell number. As the sensor of the sensor plate covers only ~55% of the well area, normalizing the OCR to the cell number in that area would reflect most closely the true OCR value / cell, while normalization to total cell number / well allows the comparison to the total protein measurements and how well total protein and total cell number are related.

The Seahorse data were analyzed using the Wave 2 software (Agilent). For all wells, the OCR curves were visually inspected for experimental issues, such as defective loading of Oligo, FCCP, or Rot/AA and wells with loading issues at any of the 3 injection stages were excluded from further analysis. The OCR curves normalized by the three different normalizations and resulting 8 quantitative parameters were exported for further graphing and statistical analysis in GraphPad Prism 8.4.3 (GraphPad Software, LLC, San Diego, CA).

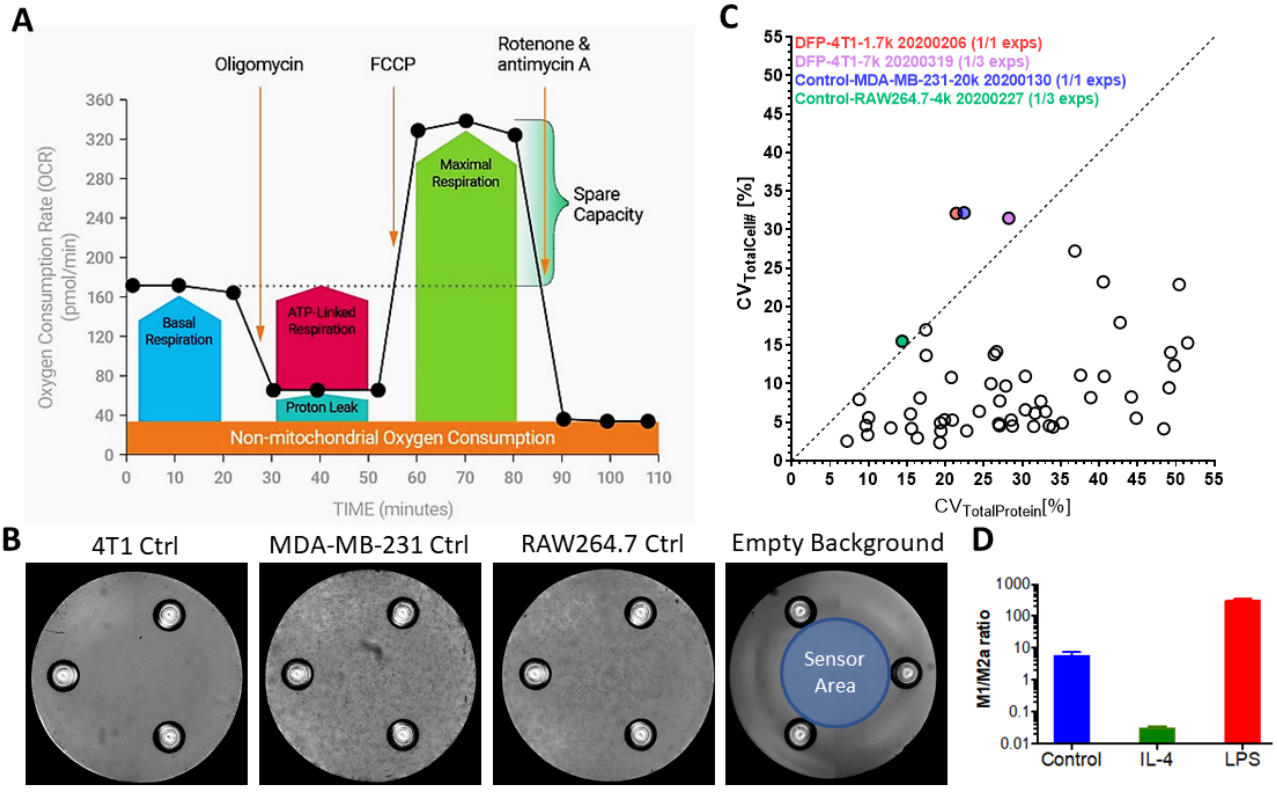

Figure 1: (**A**) Scheme of Cell Mito Stress Test and associated quantitative parameters calculated from each stage. The minimum OCR after Rot/AA injection delivers Non-Mito OC; the last rate measurement before Oligomycin injection is used to calculate the Basal Resp; the minimum OCR measurement after Oligo injection and maximum OCR measurement after FCCP injection are respectively used to calculate the remaining quantitative parameters. (**B**) Representative brightfield images of single wells with untreated cells of each cell type and an empty well. The 4 empty corner wells on the Seahorse 96-well plate serve as background controls for the Seahorse assay. The sensor area is a circular area within the three posts in each well. The differing contrast, cell density and growth homogeneity for each cell line can be discerned. (**C**) Total Protein measurements are overall more variable than Total Cell Counts. Each circle represents one experimental condition at one independent experiment with data derived from a total of 27 experimental conditions over 5 independent

(separate) experiments, leading to a total of 56 different cohorts. Only 4 of the 56 cohorts (marked in color) have a smaller Coefficient of Variation (CV) for Total Protein than for Total Cell Number. Only 3 of 56 cohorts had a similar (within <1.5%) CV for Total Protein and Total Cell Number. (**D**) 24 h exposure of RAW264.7 cells to no polarizing agent (M0), 20 ng/ml IL-4 (M2) or 100 ng/ml LPS (M1) polarization agents demonstrates the enrichment of polarized cells in cell culture. Here, the polarization to M2a was more efficient and yielded more polarized cells (33.9%±2.3%) than the polarization to M1 (22.5%±2.0%), while only few M1 (0.517%±0.094%) and M2a (0.095%±0.020%) macrophages were observed in the control (untreated, unpolarized) RAW264.7 cells (values in brackets are Mean±SE of 3 replicates of 1 experiment).

Results and Discussion

The initial 3 independent experiments aimed at establishing: (i) the seeding cell density to obtain >80% confluent cells on the day of the flux analyzer experiment and identifying if this cell number is appropriate for the mitochondrial flux analysis as well as (ii) adjust acquisition parameters such as # of measurement cycles, cycle (measurement) time and mixing time to ensure adequate reoxygenation during each measurement stage of the flux measurements. The 4T1 cells reached 100% confluence with some overgrowth in the experimental timeline due to their short doubling time and their required minimum seeding density, hindering the seeding of fewer cells to avoid overgrowth. This might affect to some extent the measurement of maximum respiration and spare respiratory capacity at the FCCP stage; nevertheless, OCR curves, normalized to total protein (data not shown), were akin to shorter experiments performed, where untreated 4T1 cells were not overgrown, resulting in similar maximum respiration and SRC [10]. As 100 µM DFP severely inhibits 4T1 proliferation, the seeding density for 4T1 cells exposed to DFP was chosen to be 7k (4.1x the seeding density of untreated 4T1 cells) to obtain a similar cell density at the time of the flux analyzer experiment for Control and DFP-exposed 4T1 cells.

We compared 3 different normalizations of OCR curves and derived quantitative parameters: OCR curves normalized to (i) Total Protein, (ii) Total Cell Number, and (iii) Total Cell Number in Sensor Area. We found that total protein does not relate very well to total cell number at high density cultures (data not shown). Additionally, the total protein measurements had a higher coefficient of variation than the total cell number measurements (**Fig. 1C**). While the results across the different normalizations are comparable (data not shown), we focus for the purpose of this report on the normalization to the total cell number in the sensor area, which we intend to use for future studies.

A representative example of OCR curves for 11 different cohorts are shown in **Figure 2**. Based on normalized OCR in the Rot/AA stage, NonMito OC (see Fig 1A above for definitions) is similar across all groups. That means that any changes in the first stage of the curves in response to DPF and/or polarization can be attributed to changes in basal respiration. As NonMito OC is similar in all experiments, the lowest values in the Oligo stage reflect H^+ Leak and ATP Prod changes, while the highest values in the FCCP stage reflect directly changes in maximal respiration and corresponding SRC.

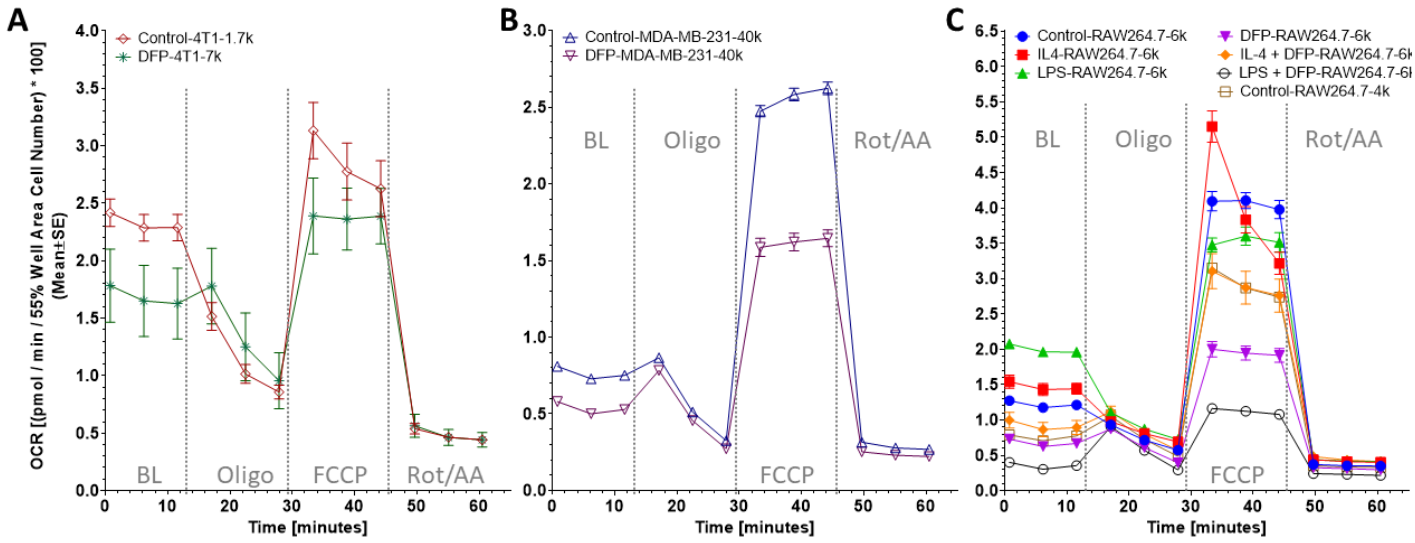

Figure 2: Oxygen Consumption Rates (OCRs) normalized to cell number in the sensor area of each well for either untreated or DFP-treated (**A**) murine TNBC cells 4T1, (**B**) human TNBC cells MDA-MB-231, and (**C**) unpolarized and polarized RAW264.7 cells. **C** also includes a RAW264.7 cell number control. Representative data from 1 of 3 experiments.

Figure 3A displays Basal Resp for the TNBC cell line cohorts as a representative example of one of the 8 quantitative parameters to visualize the inter- and intra-experimental variability from repeat experiments and replicate wells respectively. Generally, technical replication of independent experiments showed that there might be a significant

difference between mean values of different experiments or a trend that 1 of the three experiments has always higher values than the other(s). Using 2-way ANOVA, we found that for all three normalizations, group membership, experiment date and their interaction generally were significant sources of variation (P<0.0001). As there was a significant interaction between groups and experiment date, all statistical analyses of quantitative parameters (and curves) was performed paired to experiment date. Intra-experimental variability increased with decreasing cell doubling time: The cell line 4T1 with the shortest cell doubling time had typically the highest intraexperimental variability, followed by RAW264.7 (data not shown) and then MDA-MB231 cells as cell doubling times increases (**Fig. 3A**).

Figure 3B-D shows a summary for 3 of the 8 quantitative mitochondrial parameters. Group comparisons (see **Table 1-4**) were performed by 2-sided 1-way ANOVA with Geisser-Greenhouse correction and paired across experiment date. A Bonferroni post-test was applied to account for multiple comparison, with a comparison group size based on the different scientific comparisons: A) Effect of DFP on cancer cells or macrophages, B) the effect of polarization of macrophages in the presence and absence of DFP, C) as well as the comparison of the different cell types (2 TNBC cell lines and unpolarized RAW264.7 cells) in the presence and absence of DFP.

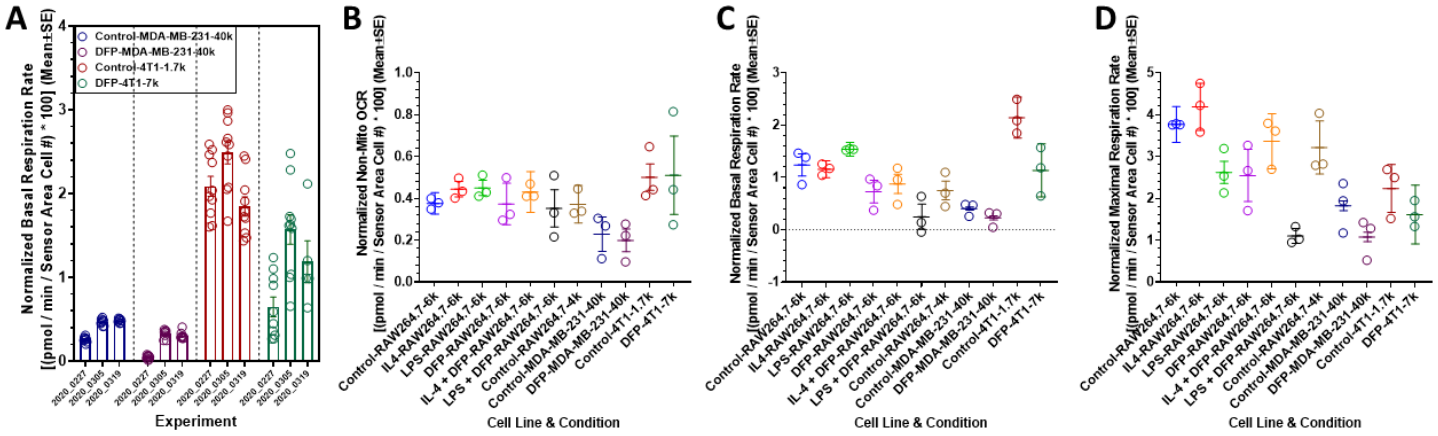

Figure 3: Selected quantitative mitochondrial parameters. (**A)** Inter- and intra-experimental variability of basal respiration of the 2 TNBC lines, untreated or DFP-treated. The bars display the mean±SE of separate experiments, while the open circles represent single wells within each experiment. (**B-D)** display the means of single experiments (open circles, n = 3) overlaid with the overall mean±SE for Non-Mito OC, Basal Resp, and Max Resp respectively. The overall SE was calculated by propagating the SD error of the means from each single experiment.

Comparing the differences between the untreated human and murine TNBC cell lines, we found that Basal Resp (**Fig. 3C**), H^+ Leak (data not shown), and ATP Prod (data not shown) are significantly higher in 4T1 than MDA-MB-231 cells, while 4T1 cells have a significantly lower % SRC (data not shown) than MDA-MB-231 cells (**Table 1, 2**). We hypothesize that the higher Basal Resp and ATP production may reflect the faster growth rate of 4T1 cells compared with MDA-MB-231 cells, or be the result of higher aerobic glycolysis in 4T1 than MDA-MB-231 contributing to total ATP turnover and cell proliferation. Nonmitochondrial oxygen consumption (**Fig. 3B**), Basal Resp (**Fig. 3C**), H^+ Leak (data not shown), ATP Prod (data not shown), and %SRC (data not shown) for untreated, unpolarized RAW264.7 cells fall somewhere between the values for the 2 TNBC lines, while Max Resp (**Fig. 3C**) and SRC (data not shown) tend to be higher in the RAW264.7 cells than in the 2 TNBC lines. These differences between the mitochondrial parameters for the 3 different cell types are diminished in the presence of DFP, consistent with reduced cell proliferation in response to DFP.

Table 1: Statistical analysis to assess the differences of NonMito OC, Basal Resp, and Max Resp between the human and murine TNBC line and the effects of DFP exposure on either. Uncorrected P values (Fisher's LSD test) color coded for Bonferroni correction, based on multiple comparison group size n to achieve 95% significance: n =2, **P ≤ 0.05**; n = 3, **P ≤ 0.0167**; n = 4, **P ≤ 0.0125**; n = 5, **P ≤ 0.01**.

TNBC Cell Line Differences in the Presence and Absence of DFP		
	NonMito OC	Basal Resp	Max Resp
Control-4T1-1.7k *vs.* Control-MDA-MB-231-40k	**0.0333**	**0.0125**	0.5012
DFP-4T1-7k *vs.* DFP-MDA-MB-231-40k	0.1115	**0.0401**	0.0722
Effect of 48 h DFP Exposure on a Human and a Murine TNBC Cell Line		
	NonMito OC	Basal Resp	Max Resp
DFP-4T1-7k *vs.* Control-4T1-1.7k	0.9236	**0.0479**	0.221

DFP-MDA-MB-231-40k *vs.* Control-MDA-MB-231-40k	0.0803	**0.011**	**0.0147**

Table 2: Statistical analysis to assess the differences of H^+ Leak, ATP Prod, SRC, and % SRC between the human and murine TNBC line and the effects of DFP exposure on either. Uncorrected P values (Fisher's LSD test) color coded for Bonferroni correction, based on multiple comparison group size n to achieve 95% significance: n =2, **P ≤ 0.05**; n = 3, **P ≤ 0.0167**; n = 4, **P ≤ 0.0125**; n = 5, **P ≤ 0.01**.

TNBC Cell Line Differences in the Presence and Absence of DFP				
	H^+ Leak	ATP Prod	SRC	% SRC
Control-4T1-1.7k *vs.* Control-MDA-MB-231-40k	**0.0141**	**0.0164**	0.1493	**0.0004**
DFP-4T1-1.7k *vs.* DFP-MDA-MB-231-40k	0.0699	**0.0152**	0.388	0.2072
Effect of 48 h DFP Exposure on a Human and a Murine TNBC Cell Line				
	H^+ Leak	ATP Prod	SRC	% SRC
DFP-4T1-7k *vs.* Control-4T1-1.7k	0.7961	**0.0201**	0.336	0.1179
DFP-MDA-MB-231-40k *vs.* Control-MDA-MB-231-40k	0.1338	**0.0204**	**0.0263**	0.4409

Nonmitochondrial oxygen consumption is not significantly affected by exposure to DFP in the 2 TNBC lines as well as unpolarized and polarized macrophages RAW264.7 cells (**Fig. 3B, Table 1, 3**), consistent with the iron chelation effect on mitochondrial, iron-dependent enzymes and corresponding effect on cell proliferation [10]. In 4T1 cells (**Fig. 3, Table 1, 2**), DFP exposure generally reduced Basal Resp (**Fig. 3C**), Max Resp (**Fig. 3D**), H^+ Leak (data not shown), and significantly ATP Production (data not shown). In MDA-MB-231 cells (**Fig. 3, Table 1, 2**), DFP exposure lowered significantly Basal Resp (**Fig. 3C**) and Max Resp (**Fig. 3D**) while it lowered NonMito OC (**Fig. 3B**), ATP Prod (data not shown), and SRC (data not shown). The DFP response observed in the TNBC lines is consistent with our observation in 3 prostate cancer lines, where 24 h DFP exposure significantly lowered Basal Resp, Max Resp, H^+ Leak (in 2 of 3 cell lines), ATP Prod (in 2 of 3 cell lines), and SRC (in 2 of 3 cell lines), while not affecting NonMitoOC [9].

In untreated, unpolarized RAW264.7 cells, DFP exhibited its largest effect on Basal Resp (**Fig. 3C**) and ATP Prod (data not shown). Generally, DFP exposure affected the mitochondrial parameters of M2 macrophages the least while in M1 macrophages the effect of DFP on mitochondrial parameters was enhanced compared to M0 and M2-polarized macrophages (**Fig. 3B-D, Table 3, 4**). Of note is that not necessarily all RAW264.7 are polarized in a population (**Fig. 1D**). The % polarization could not be assayed on the Seahorse assay samples.

In RAW264.7 cells, M2 polarization had generally no significant effect on mitochondrial parameters independent of DFP exposure. However, M1 polarization of RAW264.7 cells tended to increase Basal Resp (**Fig. 3C**), H^+ Leak (data not shown), and decrease Max Resp (**Fig. 3D**), SRC (data not shown), and % SRC (data not shown) in untreated cells, effects abrogated upon DFP exposure (**Table 3, 4**). Compared to M2 macrophages, M1 macrophages generally feature increased glycolytic and pentose phosphate pathway fluxes, accompanied by a dysfunctional Krebs (TCA) cycle [11, 12]. In M1 macrophages, citrate and succinate accumulate due to the impaired reactions catalyzed by isocitrate dehydrogenase and succinate dehydrogenase [11, 12]. The slightly higher ATP Prod in LPS-RAW264.7 cells compared with IL-4-RAW264.7 cells is consistent with ATP preferentially derived from glucose, while the higher reliance of M2 macrophages on the Krebs cycle is consistent with a higher Max Resp and SRC in M2 compared to M1 macrophages. The somewhat higher Basal Resp in M1 than in M2 macrophages might be the result of their reliance on the faster glycolysis and some modest increase in OXPHOS, similar to what has been observed in other studies [13]. This would also explain why M1 macrophages are more strongly impacted by DFP which inhibits aconitase in the TCA cycle, resulting in further accumulation of citrate and inhibition of TCA cycle, similar to our observation in prostate cancer [9].

Table 3: Statistical analysis to assess the effects of DFP on NonMito OC, Basal Resp, and Max Resp of unpolarized and polarized macrophages as well as the effects of macrophage polarization in the presence and absence of DFP. Uncorrected p values (Fisher's LSD test) color coded for Bonferroni correction, based on multiple comparison group size to achieve 95% significance: n =2, **P ≤ 0.05**; n = 3, **P ≤ 0.0167**; n = 4, **P ≤ 0.0125**; n = 5, **P ≤ 0.01**.

Effect of 48 h DFP Exposure on Unpolarized and Polarized Macrophages

	NonMito OC	Basal Resp	Max Resp
DFP-RAW264.7-6k *vs.* Control-RAW264.7-6k	0.9561	**0.0011**	0.1142
LPS + DFP-RAW264.7-6k *vs.* LPS-RAW264.7-6k (M1)	0.2193	**0.0255**	0.0669
IL-4 + DFP-RAW264.7-6k *vs.* IL4-RAW264.7-6k (M2)	0.3406	0.2218	0.324
Effect of Macrophage Polarization in the Absence of DFP			
	NonMito OC	Basal Resp	Max Resp
IL4-RAW264.7-6k *vs.* Control-RAW264.7-6k	**0.0425**	0.6148	0.3402
LPS-RAW264.7-6k *vs.* Control-RAW264.7-6k	0.0598	0.2678	0.0663
LPS-RAW264.7-6k *vs.* IL4-RAW264.7-6k	0.4241	**0.0311**	**0.0019**
Effect of Macrophage Polarization in the Presence of DFP			
	NonMito OC	Basal Resp	Max Resp
IL-4 + DFP-RAW264.7-6k *vs.* DFP-RAW264.7-6k	0.324	**0.0437**	0.0776
LPS + DFP-RAW264.7-6k *vs.* DFP-RAW264.7-6k	0.5553	0.1401	0.0552
LPS + DFP-RAW264.7-6k *vs.* IL-4 + DFP-RAW264.7-6k	0.3672	0.0843	**0.0165**

Table 4: Statistical analysis to assess the effects of DFP on H^+ Leak, ATP Prod, SRC, and % SRC of unpolarized and polarized macrophages as well as the effects of macrophage polarization in the presence and absence of DFP. Uncorrected p values (Fisher's LSD test) color coded for Bonferroni correction, based on multiple comparison group size to achieve 95% significance: n =2, **P ≤ 0.05**; n = 3, **P ≤ 0.0167**; n = 4, **P ≤ 0.0125**; n = 5, **P ≤ 0.01**.

Effect of 48 h DFP Exposure on Unpolarized and Polarized Macrophages				
	H^+ Leak	ATP Prod	SRC	% SRC
DFP-RAW264.7-6k *vs.* Control-RAW264.7-6k	**0.0358**	**0.012**	0.2598	**0.0182**
LPS + DFP-RAW264.7-6k *vs.* LPS-RAW264.7-6k	**0.0254**	**0.0451**	0.5257	0.6208
IL-4 + DFP-RAW264.7-6k *vs.* IL4-RAW264.7-6k	0.1418	0.2502	0.3834	0.4608
Effect of Macrophage Polarization in the Absence of DFP				
	H^+ Leak	ATP Prod	SRC	% SRC
IL4-RAW264.7-6k *vs.* Control-RAW264.7-6k	0.5652	0.664	0.1348	**0.0376**
LPS-RAW264.7-6k *vs.* Control-RAW264.7-6k	**0.0404**	0.3991	**0.0076**	0.0519
LPS-RAW264.7-6k *vs.* IL4-RAW264.7-6k	0.1399	0.1793	**0.0016**	**0.0201**
Effect of Macrophage Polarization in the Presence of DFP				
	H^+ Leak	ATP Prod	SRC	% SRC
IL-4 + DFP-RAW264.7-6k *vs.* DFP-RAW264.7-6k	0.1717	0.0811	0.1326	0.4563
LPS + DFP-RAW264.7-6k *vs.* DFP-RAW264.7-6k	0.1779	0.1332	0.1008	0.2831
LPS + DFP-RAW264.7-6k *vs.* IL-4 + DFP-RAW264.7-6k	**0.0499**	0.0939	**0.0052**	0.914

In summary, DFP reduced basal respiration and maximal respiration in the TNBC lines, consistent with our previous observations in prostate cancer cell lines, while the results for unpolarized and polarized RAW264.7 cells reflect the metabolic shifts between glycolysis, PPP and TCA cycle as a result of polarization in the presence and absence of intracellular iron chelation.

Further Oxygen Consumption Studies: We have learned from these studies that the faster the cell grows, the greater the intra-experimental variability for cells grown over several days. We intend to increase the number of independent experiments from 3 to 5 for the tumor cells to increase our confidence in the data. Our statistician will further review the appropriateness of the statistical analysis, since the experimental design is quite complex.

References

1. Bosiljcic, M., et al., *Targeting myeloid-derived suppressor cells in combination with primary mammary tumor resection reduces metastatic growth in the lungs.* Breast Cancer Res, 2019. **21**(1): p. 103.
2. Youn, J.I., et al., *Subsets of myeloid-derived suppressor cells in tumor-bearing mice.* J Immunol, 2008. **181**(8): p. 5791-802.
3. Galluzzi, L., et al., *Immunological Effects of Conventional Chemotherapy and Targeted Anticancer Agents.* Cancer Cell, 2015. **28**(6): p. 690-714.
4. Wanderley, C.W., et al., *Paclitaxel Reduces Tumor Growth by Reprogramming Tumor-Associated Macrophages to an M1 Profile in a TLR4-Dependent Manner.* Cancer Res, 2018. **78**(20): p. 5891-5900.
5. Zappasodi, R., et al., *Non-conventional Inhibitory CD4(+)Foxp3(-)PD-1(hi) T Cells as a Biomarker of Immune Checkpoint Blockade Activity.* Cancer Cell, 2018. **33**(6): p. 1017-1032 e7.
6. Malandro, N., et al., *Clonal Abundance of Tumor-Specific CD4(+) T Cells Potentiates Efficacy and Alters Susceptibility to Exhaustion.* Immunity, 2016. **44**(1): p. 179-193.
7. Jones, R.B., et al., *Tim-3 expression defines a novel population of dysfunctional T cells with highly elevated frequencies in progressive HIV-1 infection.* J Exp Med, 2008. **205**(12): p. 2763-79.
8. Sakuishi, K., et al., *Targeting Tim-3 and PD-1 pathways to reverse T cell exhaustion and restore anti-tumor immunity.* J Exp Med, 2010. **207**(10): p. 2187-94.
9. Simoes, R.V., et al., *Inhibition of prostate cancer proliferation by Deferiprone.* NMR Biomed, 2017. **30**(6).
10. Simoes, R.V., et al., *Metabolic plasticity of metastatic breast cancer cells: adaptation to changes in the microenvironment.* Neoplasia, 2015. **17**(8): p. 671-84.
11. Thapa, B. and K. Lee, *Metabolic influence on macrophage polarization and pathogenesis.* BMB Rep, 2019. **52**(6): p. 360-372.
12. Viola, A., et al., *The Metabolic Signature of Macrophage Responses.* Front Immunol, 2019. **10**: p. 1462.
13. Zuo, H. and Y. Wan, *Metabolic Reprogramming in Mitochondria of Myeloid Cells.* Cells, 2019. **9**(1).

The effect of iron chelation on the human TNBC MDA-MB-231 cell line – Metabolic Studies (Koutcher Laboratory)

1. Methods

1.1.1. Cells: The human, epithelial TNBC cell line MDA-MB-231 was grown in complete Dulbecco's Modified Essential (DME_{compl}) medium, containing 25 mM glucose (Glc), 6 mM glutamine (Gln), 10% fetal bovine serum and 1% penicillin/streptomycin. Cells were cultured in humidified 5% CO_2 / 95% air at 37 ºC, split every 6 to 7 days and used up to passage 10.

1.1.2. *Bioreactor Studies:* For the magnetic resonance (MR)-cell bioreactor studies, 6×10^6 MDA-MB-231 cells were seeded on microcarrier beads (0.5 ml; 125-212 µm diameter; PP3772, Corning, New York, NY) and cultured for five days, with daily medium change, in a Nunc™ Deep Form Bacteriology Petri dish (n = 7; Thermo Fisher Scientific, Pittsburgh PA, USA) until reaching ~ 70% confluence. Cell number and viability were estimated from a representative sample at the start ($\#cells_{init}$) and end ($\#cells_{end}$) of each MR experiment by Trypan Blue exclusion assay.

1.2. Monitoring Metabolism Changes: Multinuclear magnetic resonance spectroscopy (MRS)

Continually perfused, live cells were studied in an MR-compatible cell bio-reactor [9, 10] on a vertical-bore 500 MHz AVANCE III Bruker scanner equipped with a 10-mm broad-band probe (Bruker BioSpin, Billerica, MA) for ^1H and $^{31}P/^{13}C$ scans. To monitor metabolic changes, cells were continuously perfused for 31 hours with DME_{compl} media. After the setup and acquisition of the first ^{31}P MR spectrum, the un-labelled perfusion medium was replaced with DME_{compl} medium containing 25 mM 1-^{13}C-labeled glucose for the remaining 30 h of the experiment. During each experiment, ^1H-decoupled, Nuclear Overhauser Effect-enhanced ^{13}C MR spectra (1200 s relaxation time (TR), 45° flip angle, 30 kHz sweep width (SW), 8 k spectral points (np), 1000 averages, 20 min acquisition time) were acquired repetitively inter-spaced every six hours with two consecutive ^{31}P spectra (TR(repetition interval) = 1200 s, 45° flip angle, 20 kHz SW(spectral width), 2 k (np), 1800 averages, 30 min acquisition time) (**Figure 1**). Three independent experiments each, were performed in regular

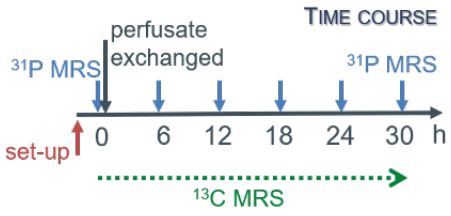

Figure 1: Experimental Schema

medium conditions (CTRL) and three in medium containing 100 µM DFP (DFP-treated). For ^{13}C and ^{31}P MR spectra an exponential line broadening of 7 Hz and 10 Hz were applied respectively before fast Fourier transformation, followed by 0 and 1st order phase correction. Quantification of MR spectral peaks was performed by time domain fitting of the metabolite signal area using AMARES (advanced method for accurate, robust and efficient spectral fitting)(jMRUI v5.2, http://www.jmrui.eu/), as described previously [10]. All metabolite signal areas were normalized to the β-NTP signal area of the first ^{31}P MR spectrum (β-NTP$_{init}$). The intra- and extra-cellular pH were calculated from the chemical shift of the respective intra- and extra-cellular inorganic phosphate (Pi) signal, as described in detail previously [10, 14].

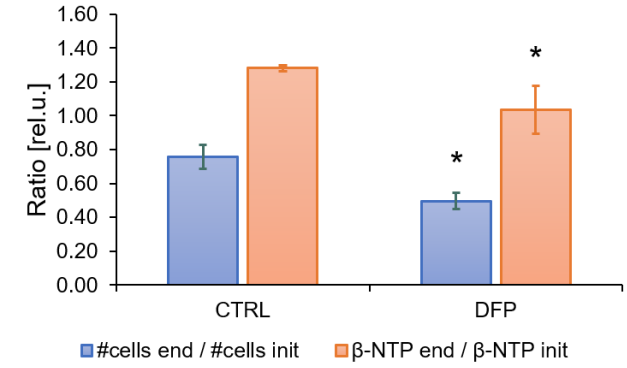

Figure 2: Cell mass and cellular energy ratio. Comparison between the ratio of the cell numbers at the end and start of the experiment (#cells $_{end}$/ # cells $_{init}$, blue bars) and the corresponding cellular energy ratio (β-NTP$_{end}$/ β-NTP$_{init}$; orange bars), calculated for both, control (CTRL) and Deferiprone (DFP)-treated MDA-MB-231 Triple Negative Breast Cancer cells. Data are mean ± standard deviation (SD), n = 3 each.
* Statistically significantly different from the corresponding values in the control (CTRL) MDA-

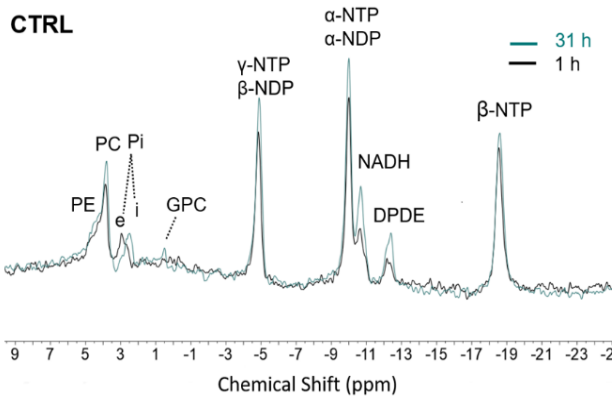

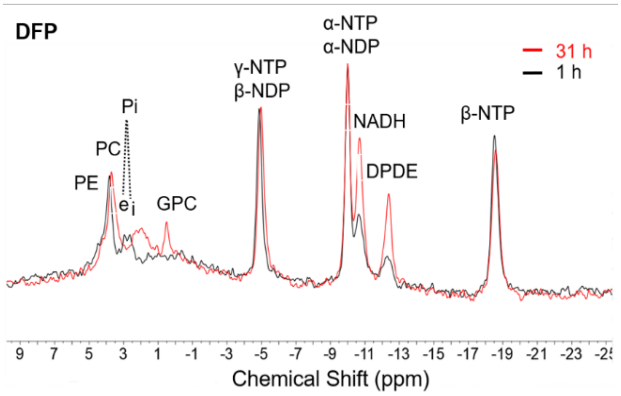

Figure 3: Representative ^{31}P MR spectra of DFP-treated and untreated MDA-MB-231 cells, depicting energy level metabolite changes over time. Top panel: Comparison between representative ^{31}P MR spectra of untreated (CTRL) MDA-MB-231 cells acquired at the start (t = 0-1 h, black spectrum) and end (t = 31 h; teal spectrum) of the experiment. **Bottom panel:** Comparison between representative ^{31}P MR spectra of DFP-treated MDA-MB-231 cells, acquired at the start (t = 0-1 h, black spectrum) and the end (t = 31 h; red spectrum) of the experiment. PE = phosphoethanolamine, PC = phosphocholine; Pi= inorganic phosphate, (e= extracellular, i = intracellular); GPC = glycerophosphocholine, NTP = nucleotide triphosphate; NDP = nucleotide diphosphate, NADH = total nicotine adenine dinucleotides and nicotine adenine dinucleotide phosphates (NAD^+, NADH, $NADP^+$, NADPH); DPDE = diphosphodiesters.

1.3. Statistical Analysis: Data were analysed using GraphPad Prism version 8.0 (GraphPad software, Inc., CA) and presented as mean ± standard error (SE), unless stated otherwise. A 2-tailed, unpaired Student's t test was used to compared DFP-treated and untreated (CTRL) MDA-MB-231 cell data. A P value < 0.05 was considered significant.

2. Results

2.1.1. Cells

2.1.2. *Cell count ratio and cellular energy ratio*

Figure 2 shows the comparison between the cell count ratios (r_C = #cells$_{end}$/#cells$_{initial}$) of each experiment and the corresponding cellular energy ratios (r_E=[β-NTP$_{end}$/β-NTP$_{init}$]) (NTP = nucleoside triphosphate) determined for both DFP-treated and untreated cells. In DFP-treated MDA-MB-231 cells, the cell mass and the cellular energy ratios were significantly lower than in untreated MDA-MB-231 cells. This agrees with our EC_{50} studies (last year's report) showing decreased proliferation and some cytotoxicity in MDA-MB-231 (EC_{50} = 58.5±5.6 µM, EC_{90} = 163±32 µM with ~50% of cells at time 0 lost after 48 h exposure to 100 µM DFP) caused by DFP. The cell loss seen in untreated MDA-MB231 cells is in line with generally occurring cell loss in nearly confluent cells observed for ≤ 1 cell doubling time (here, 31 h versus a ~40 h MDA-MB-231 doubling time). While the cell count ratio r_C decreases by 37.7±4.7% between untreated and DFP-treated MDA-MB-231 cells, the cellular energy ratio r_E decreases by 19.3±9.1%, resulting in a ~18% decrease difference (P = 0.057, 2-tailed, unpaired t test).

2.2. Assessment of Metabolism Changes by Multinuclear MRS

2.2.1. *^{31}P MRS Results & Discussion:* The comparison of representative ^{31}P spectra of DFP-treated and untreated (CTRL) MDA-MB-231 cells are respectively reported in the bottom and top panel of **Figure 3**. In each panel, spectra acquired at the start (t = 0,

black spectrum in both panels) and end (t =31 h, red spectrum for DFP-treated in the bottom panel, teal spectrum for CTRL in the top panel) of an experiment for each group of cells are reported. Spectra were analysed to measure peak ratios representing metabolite concentration ratios.

Figure 4A shows representative ^{31}P MR spectra of DFP-treated and untreated MDA-MB-231 cells acquired at 31 h. The time course of β-NTP levels is similar between DFP-treated and control MDA-MB-231 cells, except for the last two time points where β-NTP levels off in the DFP-treated cells while it keeps increasing in the untreated cells (**Figure 4B**). This observation, together with the ~18% decrease difference of r_E and r_C in response to DFP treatment (**Figure 2**), indicate not only an increase of cellular β-NTP in both, DFP-treated and untreated MDA-MB-231 cells, but also that this increase of cellular β-NTP is diminished in response to DFP. This is in line with our observation of impaired bioenergetics after 23 h of DFP exposure in TRAMP-C2 prostate cancer cells [9]. The phospholipid precursor PC (**Figure 4C**) exhibits higher values in DFP-treated than untreated MDA-MB-231 cells, with a significant difference at the earliest time point (6 h), while phosphoethanolamine (PE) is lower in DFP-treated MDA-MB-231 cells with a statistically significant difference at 18 h (**Figure 4D**). Post 6 h, the phospholipid precursor GPC increases similarly over the time frame of 31 h in DFP-treated and untreated cells (data not shown). Contrary to other treatments [14, 15] and TRAMP-C2 [9] cells, the GPC/PC ratio is increasing similarly for DFP-treated and untreated MDA-MB-231 cells at 12 h – 31 h. The difference between TRAMP-C2 and MDA-MB-231 may be in part due to the longer cell doubling of MDA-MB-231 leading to less phospholipid membrane turnover. The three phospholipid precursors PC, PE, and GPC are metabolic markers of phospholipid membrane turnover [16-18], with the higher cellular PC in DFP-treated cells possibly related to decreased phosphatidylcholine synthesis as a result of cell growth inhibition by DFP [9]. The combined signal of nicotinamide adenine dinucleotides NAD(H), and nicotinamide adenine dinucleotide phosphates NADP(H) is significantly higher in DFP-treated than untreated MDA-MB-231 cells beyond 12 h (**Figure 4E**). The intracellular pH was stable throughout and unaffected by DFP (data not shown). The extracellular pH dropped by ~ 0.19 pH units in untreated MDA-MB-231 and overlapped with DFP-treated MDA-MB-231 cells up-to 18 h, after which the intra- and extra-cellular Pi overlapped and were indistinguishable in DFP-treated cells, precluding the calculation of extracellular pH for the late time points (data not shown).

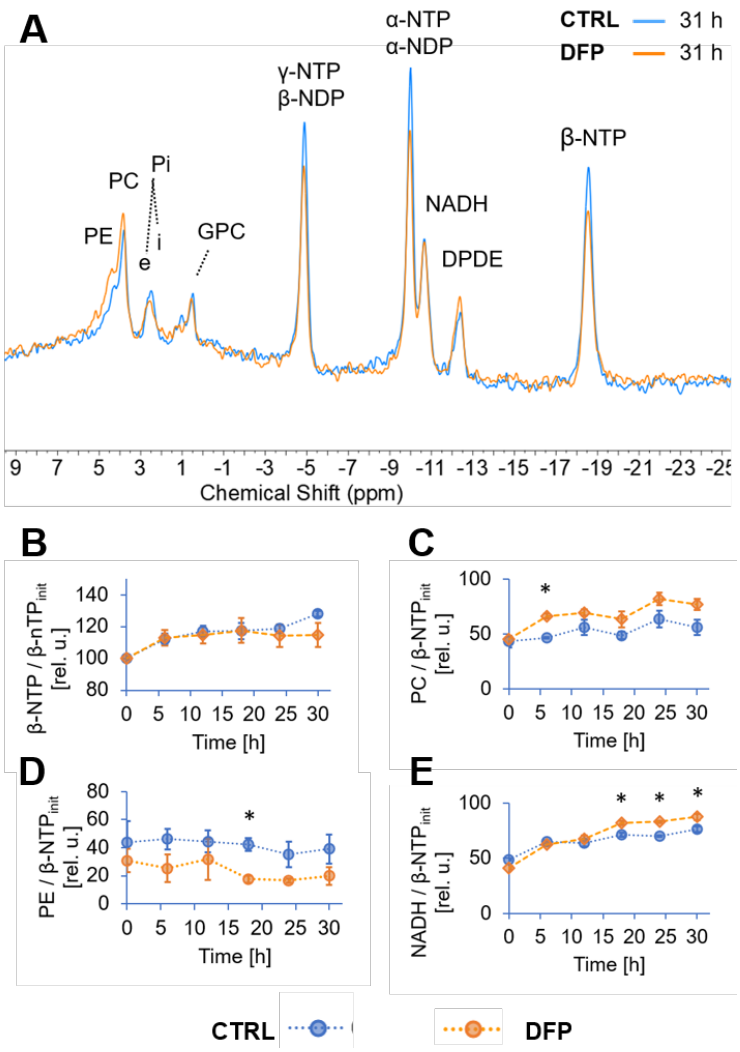

Figure 4: ^{31}P MRS results on DFP-treated and untreated MDA-MB-231 cells. **A:** Representative ^{31}P spectra of DFP-treated (red spectrum) and untreated MDA-MB-231 cells (CTRL; blue spectrum), acquired at 31 h. **B, C, D, E**: Time course of selected metabolites: β-NTP (**B**), PC (**C**), PE (**D**) and NADH, i.e. the combined signals of NAD^+, $NADP^+$ NADH, NADPH (**E**). *Statistically significantly different from the corresponding values in control (CTRL) MDA-MB-231 cells ($P < 0.05$).

2.2.2. ***^{13}C MRS Results & Discussion***: Figure 5 shows representative ^{13}C MR spectra of DFP-treated (bottom panel) and untreated (CTRL) MDA-MB-231 cells (top panel), acquired at the start (t = 1 h; black spectrum in both panels) and the end (31 h; red spectrum for DFP treated in the bottom panel and teal spectrum for CTRL in the top panel) of a representative experiment. A direct comparison between ^{13}C MR spectra of DFP-treated (orange spectrum) and untreated MDA-MB-231 cells (CTRL, blue spectrum) at 31 h is shown in Figure 6.

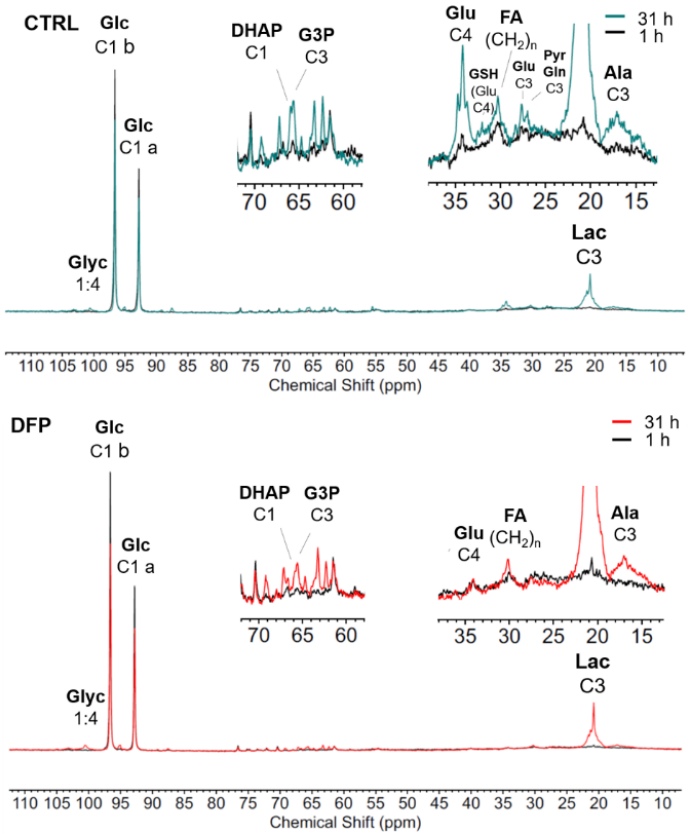

Figure 5: Representative ^{13}C MR spectra of DFP-treated and untreated MDA-MB-231 cells.
Top Panel: Comparison between representative ^{13}C MR spectra of untreated (CTRL) MDA-MB-231 cells acquired at the start (t = 0 h, black spectrum) and end (t = 31 h; teal spectrum) of the experiment. **Bottom panel:** Comparison between representative ^{13}C MR spectra of DFP-treated MDA-MB-231 cells, acquired at the start (t = 0 h, black line) and the end (t = 31 h; red line) of an experiment. Glyc = glycogen; Glc = glucose; DHAP = dihydroxyacetone phosphate; G3P = glycerol-3-phosphate; Glu = glutamate; FA = fatty acids; GSH = glutathione; Pyr = pyruvate, Ala = alanine.

The quantitative evaluation of ^{13}C spectra metabolites of DFP-treated and control MDA-MB-231 cells (**Figure 7A**) shows various average metabolite levels that significantly differ between DFP-treated and untreated MDA-MB-231 cells. The dynamic **^{13}C MRS** monitoring of MDA-MB-231 cells while perfused with 1-^{13}C-glucose (Glc) allows the evaluation of metabolic changes induced by DFP treatment (**Figure 7B**). A significant decrease in uptake and metabolism of Glc 1Cα and Glc 1Cβ respectively were observed in the presence of DFP at 12 h and 18 h of perfusion for Glc 1Cα and at 12 h – 31 h of perfusion for Glc 1Cβ. At the same time, the incorporation of Glc into glycogen (Glyc) is significantly higher in DFP-treated than untreated MDA-MB-231 cells while de-novo glutamate (Glu) synthesis significantly decreases in DFP-treated compared to untreated MDA-MB-231 cells (**Figure 7B**). Along the whole experiment (31 h), levels of dihydroxyacetone phosphate (DHAP), glycerol-3-phosphate (G3P) and alanine (Ala) do not show significant differences between DFP-treated and untreated MDA-MB-231 cells while the lactate labelling rate is significantly lower in DFP-treated than untreated MDA-MB-231 cells at each time point (**Figure 7**). These data suggest a decrease both in glycolysis (decreased lactate), Krebs cycle activity (decreased C4 glutamate), decreased overall glucose utilization, and decreased phosphatidylcholine synthesis as a result of cell growth inhibition by DFP. The combined signal of nicotinamide adenine dinucleotides NAD(H), and nicotinamide adenine dinucleotide phosphates NADP(H) is significantly higher in DFP-treated than untreated MDA-MB-231 cells beyond 12 h (**Figure 4E**), which would require further studies of the PPP to probe these changes.

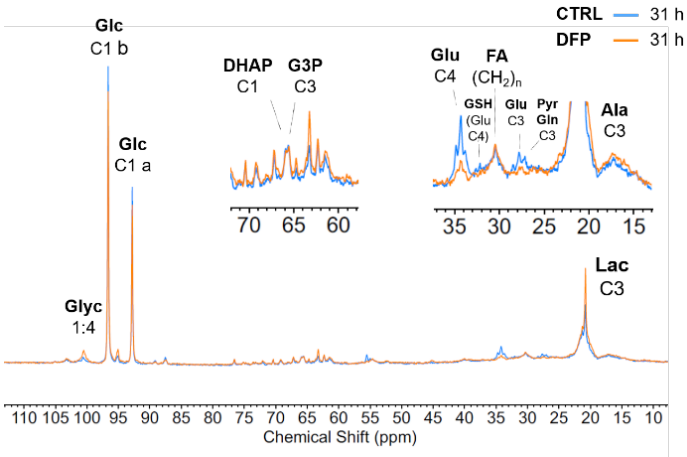

Figure 6: Representative ^{13}C MR spectra of DFP-treated and untreated MDA-MB-231 cells acquired at 31 h.
Comparison between ^{13}C MR spectra acquired at 31 h on DFP-treated (orange spectrum) and untreated (CTRL) MDA-MB-231 cells (blue spectrum). Peak assignments are the same as in **Figure 5**.

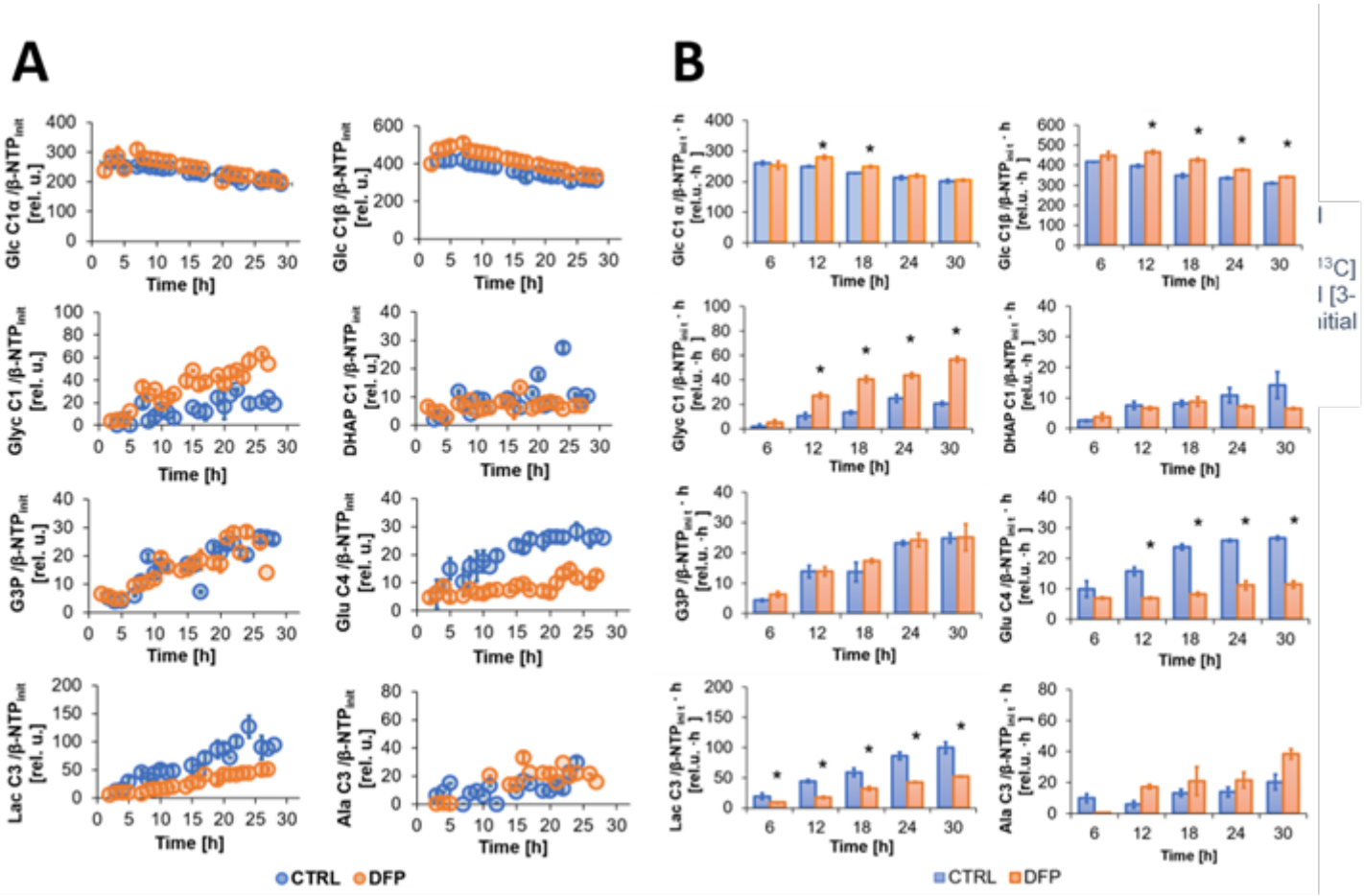

References

1. Bosiljcic, M., et al., *Targeting myeloid-derived suppressor cells in combination with primary mammary tumor resection reduces metastatic growth in the lungs.* Breast Cancer Res, 2019. **21**(1): p. 103.
2. Youn, J.I., et al., *Subsets of myeloid-derived suppressor cells in tumor-bearing mice.* J Immunol, 2008. **181**(8): p. 5791-802.
3. Galluzzi, L., et al., *Immunological Effects of Conventional Chemotherapy and Targeted Anticancer Agents.* Cancer Cell, 2015. **28**(6): p. 690-714.
4. Wanderley, C.W., et al., *Paclitaxel Reduces Tumor Growth by Reprogramming Tumor-Associated Macrophages to an M1 Profile in a TLR4-Dependent Manner.* Cancer Res, 2018. **78**(20): p. 5891-5900.
5. Zappasodi, R., et al., *Non-conventional Inhibitory CD4(+)Foxp3(-)PD-1(hi) T Cells as a Biomarker of Immune Checkpoint Blockade Activity.* Cancer Cell, 2018. **33**(6): p. 1017-1032 e7.
6. Malandro, N., et al., *Clonal Abundance of Tumor-Specific CD4(+) T Cells Potentiates Efficacy and Alters Susceptibility to Exhaustion.* Immunity, 2016. **44**(1): p. 179-193.
7. Jones, R.B., et al., *Tim-3 expression defines a novel population of dysfunctional T cells with highly elevated frequencies in progressive HIV-1 infection.* J Exp Med, 2008. **205**(12): p. 2763-79.
8. Sakuishi, K., et al., *Targeting Tim-3 and PD-1 pathways to reverse T cell exhaustion and restore anti-tumor immunity.* J Exp Med, 2010. **207**(10): p. 2187-94.
9. Simoes, R.V., et al., *Inhibition of prostate cancer proliferation by Deferiprone.* NMR Biomed, 2017. **30**(6).
10. Simoes, R.V., et al., *Metabolic plasticity of metastatic breast cancer cells: adaptation to changes in the microenvironment.* Neoplasia, 2015. **17**(8): p. 671-84.
11. Thapa, B. and K. Lee, *Metabolic influence on macrophage polarization and pathogenesis.* BMB Rep, 2019. **52**(6): p. 360-372.
12. Viola, A., et al., *The Metabolic Signature of Macrophage Responses.* Front Immunol, 2019. **10**: p. 1462.
13. Zuo, H. and Y. Wan, *Metabolic Reprogramming in Mitochondria of Myeloid Cells.* Cells, 2019. **9**(1).
14. Ackerstaff, E., et al., *Anti-inflammatory agent indomethacin reduces invasion and alters metabolism in a human breast cancer cell line.* Neoplasia, 2007. **9**(3): p. 222-35.

15. Glunde, K., et al., *Real-time changes in ^{1}H and ^{31}P NMR spectra of malignant human mammary epithelial cells during treatment with the anti-inflammatory agent indomethacin.* Magn Reson Med, 2002. **48**(5): p. 819-25.
16. Ackerstaff, E., K. Glunde, and Z.M. Bhujwalla, *Choline phospholipid metabolism: a target in cancer cells?* J Cell Biochem, 2003. **90**(3): p. 525-33.
17. Glunde, K., et al., *Choline phospholipid metabolism in cancer: consequences for molecular pharmaceutical interventions.* Mol Pharm, 2006. **3**(5): p. 496-506.
18. Kent, C., *Eukaryotic phospholipid biosynthesis.* Annu Rev Biochem, 1995. **64**: p. 315-43.

What opportunities for training and professional development has the project provided?

If the project was not intended to provide training and professional development opportunities or there is nothing significant to report during this reporting period, state "Nothing to Report."

Describe opportunities for training and professional development provided to anyone who worked on the project or anyone who was involved in the activities supported by the project. "Training" activities are those in which individuals with advanced professional skills and experience assist others in attaining greater proficiency. Training activities may include, for example, courses or one-on-one work with a mentor. "Professional development" activities result in increased knowledge or skill in one's area of expertise and may include workshops, conferences, seminars, study groups, and individual study. Include participation in conferences, workshops, and seminars not listed under major activities.

This was not a training grant so there is nothing to report. Nevertheless in Year 1 this supported Dr. Leftin who went on to write his own peer reviewed funding based on experiments begun under the auspices of this proposal and now has a faculty job at SUNY Stony Brook. He used his training on iron studies and metabolism to advance to a full time tenure track position. Dr. Porcari has been working on this project and is a postdoctoral fellow and has gone to two conferences to present findings from this project.

How were the results disseminated to communities of interest?

If there is nothing significant to report during this reporting period, state "Nothing to Report."
Describe how the results were disseminated to communities of interest. Include any outreach activities that were undertaken to reach members of communities who are not usually aware of these project activities, for the purpose of enhancing public understanding and increasing interest in learning and careers in science, technology, and the humanities.

1. Porcari P, Ackerstaff E, Winkleman DP, Veeraperumal S, Kruchevsky N, Lekaye HC, Koutcher JA. **The Role of Iron Chelation in the Tumour Microenvironment of Triple-Negative Breast Cancer**. 28th ISMRM Annual Meeting, Virtual Conference 2020, August 8-14. Oral Presentation, 0144.
(selected for presentation at the **Cancer Imaging Highlights Sessions** of the ISMRM 2020).
"Iron Chelation Affects Cell Growth and Metabolism in the Triple-negative Breast Cancer Cell Line 4T1" Porcari P, LeKaye HC, Koutcher JA, Ackerstaff E. World Molecular Imaging Congress 2019, September 4-7, Montreal, Canada. Poster presentation, P300

What do you plan to do during the next reporting period to accomplish the goals?

If this is the final report, state "Nothing to Report."
Describe briefly what you plan to do during the next reporting period to accomplish the goals and objectives.

1. The effect of DFP on enhancing efficacy of PD-1 antibodies in vivo (**Blasberg, Koutcher Lab**)
2. The effect of DFP on MDA-MB-231 on tumor growth delay, as a single agent and in combination with cisplatin and paclitaxel (**Koutcher Lab**)
3. Migration assay for MDA-MB-231 (**Koutcher Lab**)

4. **IMPACT:** D*escribe distinctive contributions, major accomplishments, innovations, successes, or any change in practice or behavior that has come about as a result of the project relative to:*

What was the impact on the development of the principal discipline(s) of the project?
If there is nothing significant to report during this reporting period, state "Nothing to Report."

Describe how findings, results, techniques that were developed or extended, or other products from the project made an impact or are likely to make an impact on the base of knowledge, theory, and research in the principal disciplinary field(s) of the project. Summarize using language that an intelligent lay audience can understand (Scientific American style).

In view of the fact that DFP is in clinical use, our most significant finding was that it enhanced immune response in the 4T1 murine TNBC, a tumor that is known to be immunologically "cold" (relatively inactive). We found that in the spleen 1) DFP increased the percent of CD4 and CD8 effector T cells, 2) enhanced these cell numbers when used in combination with cisplatin, 3) decreased cells that expressed high level of the inhibitory PD-1 receptor, indicating a shift to a pro-inflammatory environment, and a decrease in immune suppressive cells. In both spleen and tumor, DFP induced an increase in the ability of CD4 and CD8 T cells to make both IFNγ or TNFα, a marker of polyfunctionality in T cells. DFP induced an increase in cells that made either IFNγ or TNFα. There was a decrease in effector memory (T-EM, defined as CD44+CD62L-) CD8 T cells, which was coupled with an increase in the long-lived central memory (T-CM defined as CD44+CD62L+) CD8 T cells.

What was the impact on other disciplines?
If there is nothing significant to report during this reporting period, state "Nothing to Report."

Describe how the findings, results, or techniques that were developed or improved, or other products from the project made an impact or are likely to make an impact on other disciplines.

Nothing to report

What was the impact on technology transfer?
If there is nothing significant to report during this reporting period, state "Nothing to Report."

Describe ways in which the project made an impact, or is likely to make an impact, on commercial technology or public use, including:

- *transfer of results to entities in government or industry;*
- *instances where the research has led to the initiation of a start-up company; or*
- *adoption of new practices.*

Nothing to report

What was the impact on society beyond science and technology?
If there is nothing significant to report during this reporting period, state "Nothing to Report."

Describe how results from the project made an impact, or are likely to make an impact, beyond the bounds of science, engineering, and the academic world on areas such as:

- *improving public knowledge, attitudes, skills, and abilities;*
- *changing behavior, practices, decision making, policies (including regulatory policies), or social actions; or*
- *improving social, economic, civic, or environmental conditions.*

In year 2, we have shown that MRI can be used to measure and quantitate iron in vivo. This MAY go to clinical use (**Koutcher Lab**). Otherwise, nothing to report.

5. CHANGES/PROBLEMS: *The PD/PI is reminded that the recipient organization is required to obtain prior written approval from the awarding agency grants official whenever there are significant changes in the project or its direction. If not previously reported in writing, provide the following additional information or state, "Nothing to Report," if applicable:*

Changes in approach and reasons for change
Describe any changes in approach during the reporting period and reasons for these changes. Remember that significant changes in objectives and scope require prior approval of the agency.

Not applicable – nothing to report

Actual or anticipated problems or delays and actions or plans to resolve them
Describe problems or delays encountered during the reporting period and actions or plans to resolve them.

COVID-19 had a major impact. The laboratories were shut down for two months and a key person was stuck overseas. Fortunately, she had a computer and data to analyze but being away 6 months was a major loss to this project. Thus, the analysis of the metabolism studies on MDA-MB-231 which where the data were acquired in 12/19-3/20 were just completed and not truly digested in terms of biochemical significance. We will work further on that in the coming months and present the data at meetings after further consideration of the significance.

Changes that had a significant impact on expenditures
Describe changes during the reporting period that may have had a significant impact on expenditures, for example, delays in hiring staff or favorable developments that enable meeting objectives at less cost than anticipated.

Loss of technician in year 2 for about 8 months has allowed us to carry funds over to a no cost extension year. Gap in postdoctoral fellows due to recruiting an experienced person from overseas has also allowed carry over of funds which is necessary to complete the studies due to these delays.

Significant changes in use or care of human subjects, vertebrate animals, biohazards, and/or select agents
Describe significant deviations, unexpected outcomes, or changes in approved protocols for the use or care of human subjects, vertebrate animals, biohazards, and/or select agents during the reporting period. If required, were these changes approved by the applicable institution committee (or equivalent) and reported to the agency? Also specify the applicable Institutional Review Board/Institutional Animal Care and Use Committee approval dates.

Significant changes in use or care of human subjects

No human subjects

Significant changes in use or care of vertebrate animals

No change in vertebrate animals

Significant changes in use of biohazards and/or select agents

None

6. PRODUCTS:

- **Publications, conference papers, and presentations**
  Report only the major publication(s) resulting from the work under this award.

1. "The Role of Iron Chelation in the Tumour Microenvironment of Triple-Negative Breast Cancer"
Porcari P, Ackerstaff E, Winkleman DP, Veeraperumal S, Kruchevsky N, Lekaye HC, Koutcher JA
28th ISMRM Annual Meeting, Virtual Conference 2020, August 8-14. Oral Presentation, 0144.

The abstract was selected for presentation at the **Cancer Imaging Highlights Sessions** of the ISMRM 2020.

2. "Iron Chelation Affects Cell Growth and Metabolism in the Triple-negative Breast Cancer Cell Line 4T1" Porcari P, LeKaye HC, Koutcher JA, Ackerstaff E. World Molecular Imaging Congress 2019, September 4-7, Montreal, Canada. Poster presentation, P300

Journal publications. *List peer-reviewed articles or papers appearing in scientific, technical, or professional journals. Identify for each publication: Author(s); title; journal; volume: year; page numbers; status of publication (published; accepted, awaiting publication; submitted, under review; other); acknowledgement of federal support (yes/no).*

None during this period.

Books or other non-periodical, one-time publications. *Report any book, monograph, dissertation, abstract, or the like published as or in a separate publication, rather than a periodical or series. Include any significant publication in the proceedings of a one-time conference or in the report of a one-time study, commission, or the like. Identify for each one-time publication: author(s); title; editor; title of collection, if applicable; bibliographic information; year; type of publication (e.g., book, thesis or dissertation); status of publication (published; accepted, awaiting publication; submitted, under review; other); acknowledgement of federal support (yes/no).*

None.

Other publications, conference papers and presentations. *Identify any other publications, conference papers and/or presentations not reported above. Specify the status of the publication as noted above. List presentations made during the last year (international, national, local societies, military meetings, etc.). Use an asterisk (*) if presentation produced a manuscript.*

None.

- **Website(s) or other Internet site(s)**
  List the URL for any Internet site(s) that disseminates the results of the research activities. A short description of each site should be provided. It is not necessary to include the publications already specified above in this section.

None.

- **Technologies or techniques**
  Identify technologies or techniques that resulted from the research activities. Describe the technologies or techniques were shared.

None in Year 3.

- **Inventions, patent applications, and/or licenses**
  Identify inventions, patent applications with date, and/or licenses that have resulted from the research. Submission of this information as part of an interim research performance progress report is not a substitute for any other invention reporting required under the terms and conditions of an award.

None in Year 3.

- **Other Products**

  Identify any other reportable outcomes that were developed under this project. Reportable outcomes are defined as a research result that is or relates to a product, scientific advance, or research tool that makes a meaningful contribution toward the understanding, prevention, diagnosis, prognosis, treatment and /or rehabilitation of a disease, injury or condition, or to improve the quality of life. Examples include:

  - *data or databases;*
  - *physical collections;*
  - *audio or video products;*
  - *software;*
  - *models;*
  - *educational aids or curricula;*
  - *instruments or equipment;*
  - *research material (e.g., Germplasm; cell lines, DNA probes, animal models);*
  - *clinical interventions;*
  - *new business creation; and*
  - *other.*

None

7. PARTICIPANTS & OTHER COLLABORATING ORGANIZATIONS

What individuals have worked on the project?

Participants:

<u>Koutcher Laboratory; W81XWH-17-1-0525 (Initiating PI)</u>

Jason Koutcher; Corresponding PI, 9.3% (1.2 months); Dr. Koutcher directs the overall project. Funding Support – NIH

Ellen Ackerstaff ~38% - (Co-Investigator) Dr. Ackerstaff supervises all the metabolic studies performed both in vivo and in vitro. Other support – NIH

Soe Min – 50% - she takes the place of Ms. Kruchevsky and provides technical support (cell studies and in vivo studies

Paola Porcari = 50% - postdoctoral fellow; performs all the MR studies and some cell studies

<u>Blasberg Laboratory; W81XWH-17-1-0526 (Partnering PI)</u>

Ronald Blasberg: Supporting PI; 10% (1.2 months); Dr. Blasberg directs/supervises many of the cell studies including oxygen consumption measurements, proliferation etc

Taha Merghoub; Co-Investigator (Co-I) 10% (~ 1 month) – supervises flow cytometry and immune studies

Sadna Budhu – Co-Investigator – 20% - 2.4 calendar months - performs the flow cytometry and immune studies to monitor the effect of DFP on immune cells; Other support - NIH

Has there been a change in the active other support of the PD/PI(s) or senior/key personnel since the last reporting period?
If there is nothing significant to report during this reporting period, state "Nothing to Report."

If the active support has changed for the PD/PI(s) or senior/key personnel, then describe what the change has been. Changes may occur, for example, if a previously active grant has closed and/or if a previously pending grant is now active. Annotate this information so it is clear what has changed from the previous submission. Submission of other support information is not necessary for pending changes or for changes in the level of effort for active support reported previously. The awarding agency may require prior written approval if a change in active other support significantly impacts the effort on the project that is the subject of the project report.

See below.

KOUTCHER, JASON
Nothing to report.

BLASBERG, RONALD
Nothing to report.

MERGHOUB, TAHA

(NEW)
4 U01 CA224175-04 (PI: Balachandran / Leach) 9/1/2020 - 8/31/2022 0.60 calendar
NCI
Defining neoantigen immunodominance for antigen selection and biomarker discovery in human pancreatic cancer immunotherapy
This proposal uses tumor DNA detected in blood and tissue biopsies to study how the immune system recognizes pancreatic cancer. Our goal is to use these tools to identify pancreatic cancer patients most suitable for immunotherapies.
Role: Co-Investigator

(NEW)
R01 CA242069-01A1 (PI: Cerchietti) 12/1/2019 - 11/30/2024 0.60 calendar
NCI
ROLE OF THE STROMAL MICROENVIRONMENT IN B-CELL LYMPHOMA PROGRESSION AND IMMUNE ESCAPE
The purpose of our studies is to identify novel therapeutic vulnerabilities for a common type of aggressive lymphoma (diffuse large B-cell lymphoma) by understanding the role of lymphoma associated fibroblasts that are part of the tumor microenvironment. We will determine the mechanisms that fibroblasts utilize to sustain lymphoma cell grow and to decrease the lymphoma immune response.
Role: Principal Investigator

(NEW)
GC260131 (PI: Greenbaum) 5/1/2020 - 12/31/2021 0.60 calendar
Stand Up To Cancer
Computational Deconstruction of Neoantigen-TCR Degeneracy for Cancer Immunotherapy
Aim 1: Define the rules of recognition of cancer neoantigens by human T cells. Aim 2: Identify the role of the host microbiome in modulating neoantigen recognition. Aim 3: Evaluate a neoantigen cancer vaccine as an adjuvant pancreatic cancer therapy.
Role: Co-Investigator

(NEW)

W81XWH2010723 (PI: Merghoub) 9/1/2020 - 8/31/2024 Congressionally Directed Medical Research Programs 0.60 calendar
Mechanism-based approach for combination therapies with immune modulation for management of patients with urothelial cancers of the upper urinary tract
1. To perform genomic, transcriptional, and spatial assessment of the native, pre-treatment tumor and immune landscape in UTUC. 2. To evaluate the correlation of tissue samples with urine samples. 3. To determine the effect of therapeutic treatment on immune response.
Role: Principal Investigator

ACKERSTAFF, ELLEN
Nothing to report.

What other organizations were involved as partners?
If there is nothing significant to report during this reporting period, state "Nothing to Report."

Describe partner organizations – academic institutions, other nonprofits, industrial or commercial firms, state or local governments, schools or school systems, or other organizations (foreign or domestic) – that were involved with the project. Partner organizations may have provided financial or in-kind support, supplied facilities or equipment, collaborated in the research, exchanged personnel, or otherwise contributed.

Provide the following information for each partnership:
Organization Name:
Location of Organization: (if foreign location list country)
Partner's contribution to the project (identify one or more)

- *Financial support;*
- *In-kind support (e.g., partner makes software, computers, equipment, etc., available to project staff);*
- *Facilities (e.g., project staff use the partner's facilities for project activities);*
- *Collaboration (e.g., partner's staff work with project staff on the project);*
- *Personnel exchanges (e.g., project staff and/or partner's staff use each other's facilities, work at each other's site); and*
- *Other.*

None.

8. SPECIAL REPORTING REQUIREMENTS

COLLABORATIVE AWARDS: *For collaborative awards, independent reports are required from BOTH the Initiating Principal Investigator (PI) and the Collaborating/Partnering PI. A duplicative report is acceptable; however, tasks shall be clearly marked with the responsible PI and research site. A report shall be submitted to* ***https://ers.amedd.army.mil*** *for each unique award.*

QUAD CHARTS: *If applicable, the Quad Chart (available on https://www.usamraa.army.mil) should be updated and submitted with attachments.*

9. APPENDICES: *Attach all appendices that contain information that supplements, clarifies or supports the text. Examples include original copies of journal articles, reprints of manuscripts and abstracts, a curriculum vitae, patent applications, study questionnaires, and surveys, etc.*